Electronic Supplementary Information

Adsorption enhancement of nitrogen gas by atomically heterogeneous nanospace of boron nitride

Jun Kimura,[a] Takahiro Ohkubo, *[a] Yuta Nishina,[b] Koki Urita [c] and Yasushige Kuroda [a]

[a] Department of Chemistry, Graduate School of Natural Science and Technology, Okayama University, 3-1-1 Tsushima, Kita-ku, Okayama 700-8530, Japan.

[b] Research Core for Interdisciplinary Sciences, Okayama University, 3-1-1 Tsushima, Kita-ku, Okayama 700-8530, Japan.

[c] Graduate School of Engineering, Nagasaki University, 1-14 Bunkyo-machi, Nagasaki, Nagasaki 852-8521, Japan

Materials and Methods

To compare the stability to the oxidation of p-BN under the atmospheric condition, we calcined each p-BN. Calcined p-BN samples were heat-treated at 973 K under the atmosphere. The heating rate and the keeping time at the maximum temperature were fixed at 10 K/min. and 1 h, respectively. The calcined samples thus obtained are denoted as p-BN-*x*-ox.

The IR spectra were collected using a DIGILAB FTS4000MXK spectrophotometer. Each powdered p-BN sample was pressed along with KBr to make pellets. The spectra were then measured under atmospheric conditions. Pore-size distributions of p-BN samples were obtained from the adsorption branches of N_2 isotherms by using the pre-installed software in the BELSORP-max system where a carbon slit-shaped pore model in the nonlocal density functional theory (NLDFT) code was approximately selected. SEM observations were carried out by S-5200 (Hitachi Corp.). Electron accelerating voltage was fixed at 20 kV.

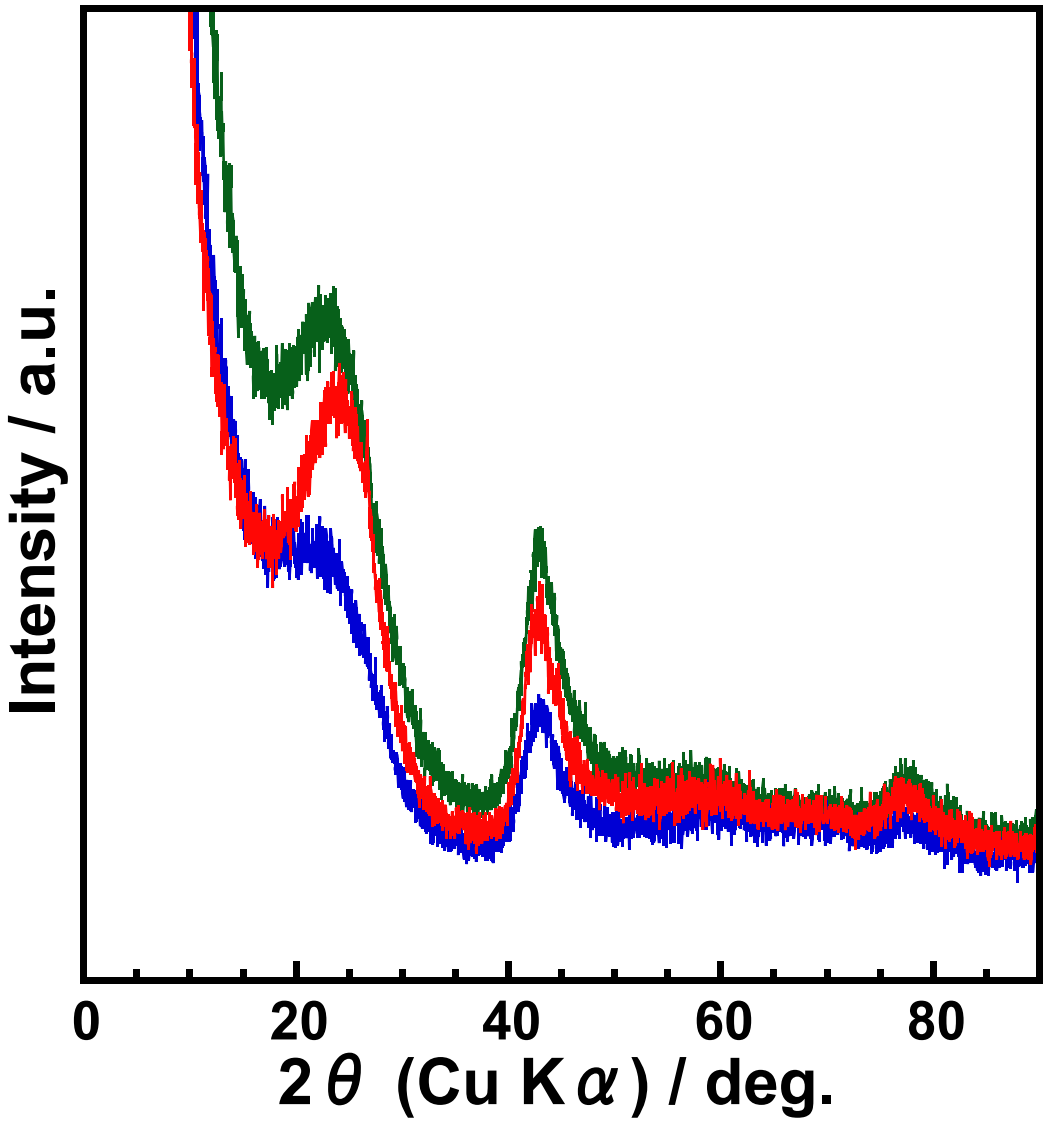

Fig. S1 Powder XRD profiles of p-BN-1473 (green), p-BN-1573 (blue) and p-BN-1673 (red).

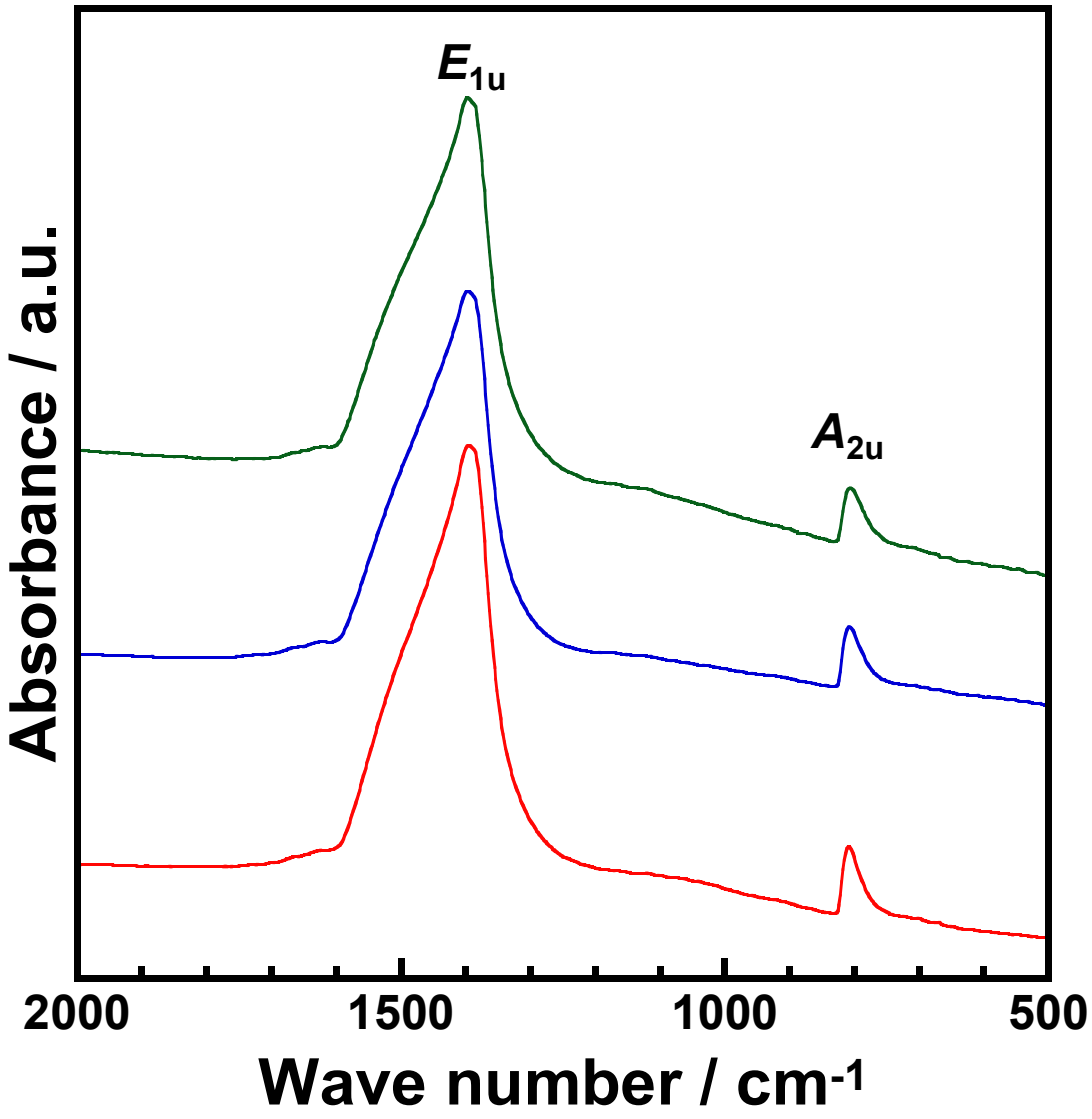

Fig. S2 IR spectra of p-BN-1473 (green), p-BN-1573 (blue) and p-BN-1673 (red).

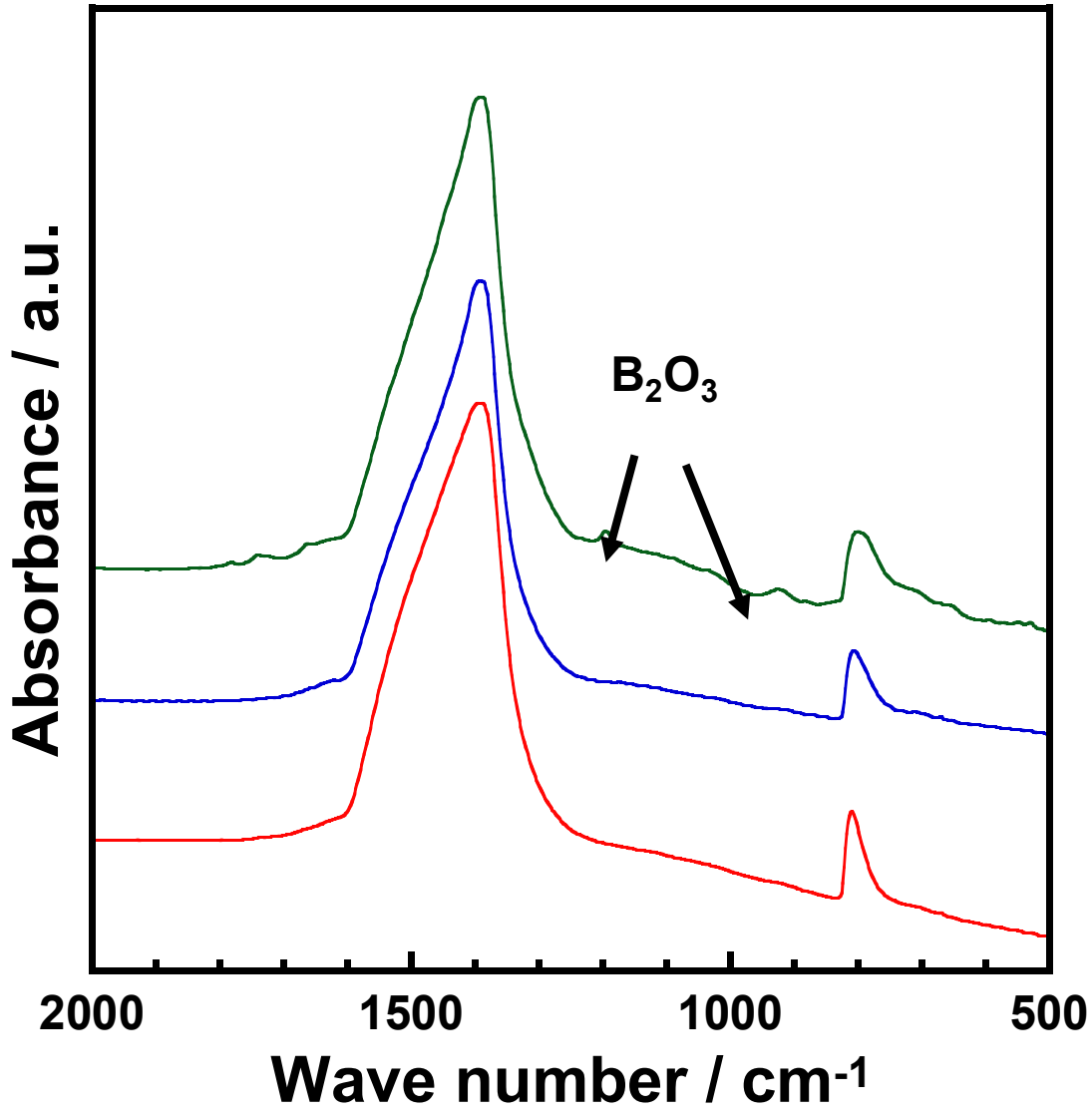

Fig. S3 IR spectra of p-BN-1473-ox (green), p-BN-1573-ox (blue) and p-BN-1673-ox (red).

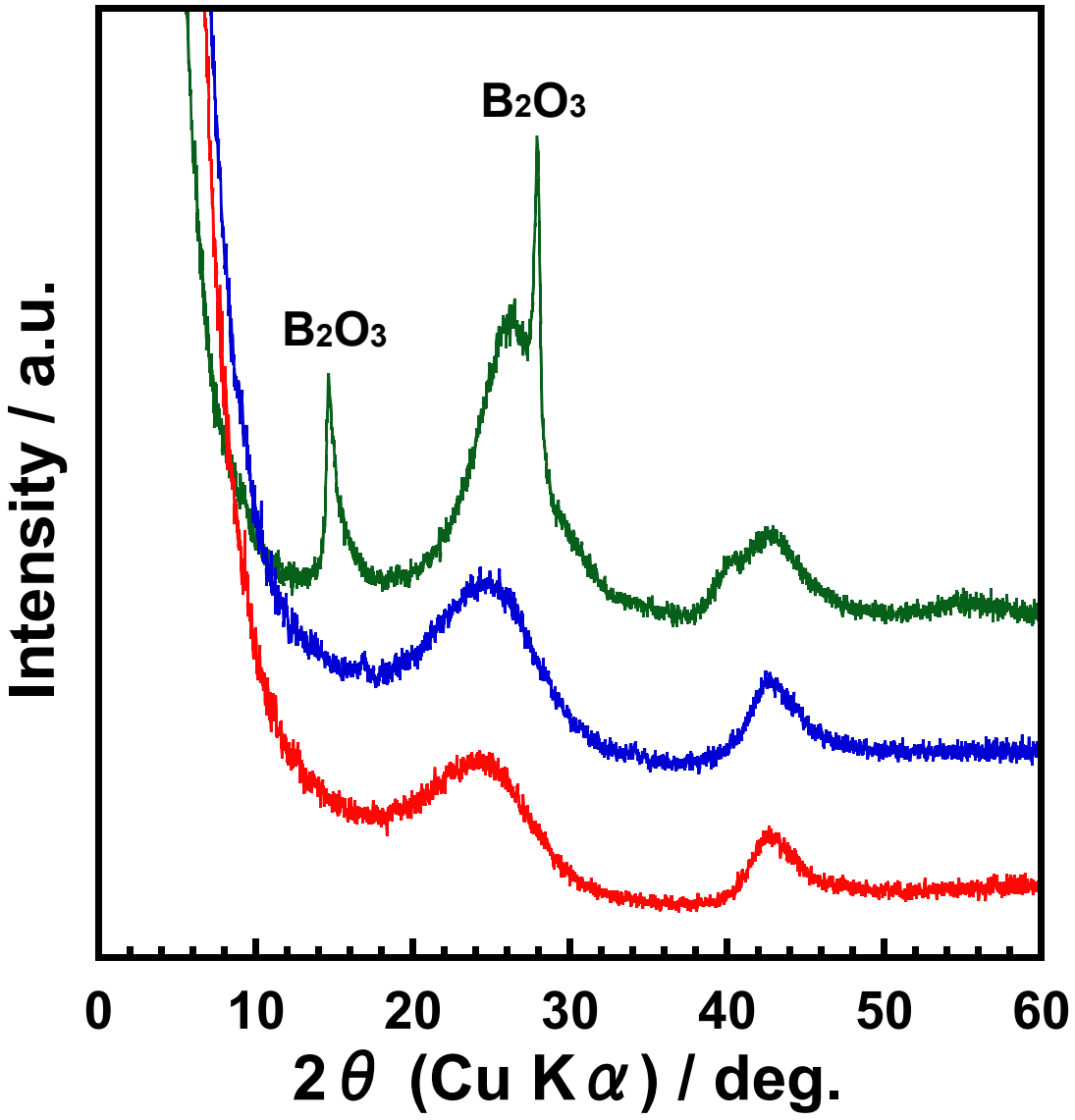

Fig. S4 Powder XRD profiles of p-BN-1473-ox (green), p-BN-1573-ox (blue) and p-BN-1673-ox (red).

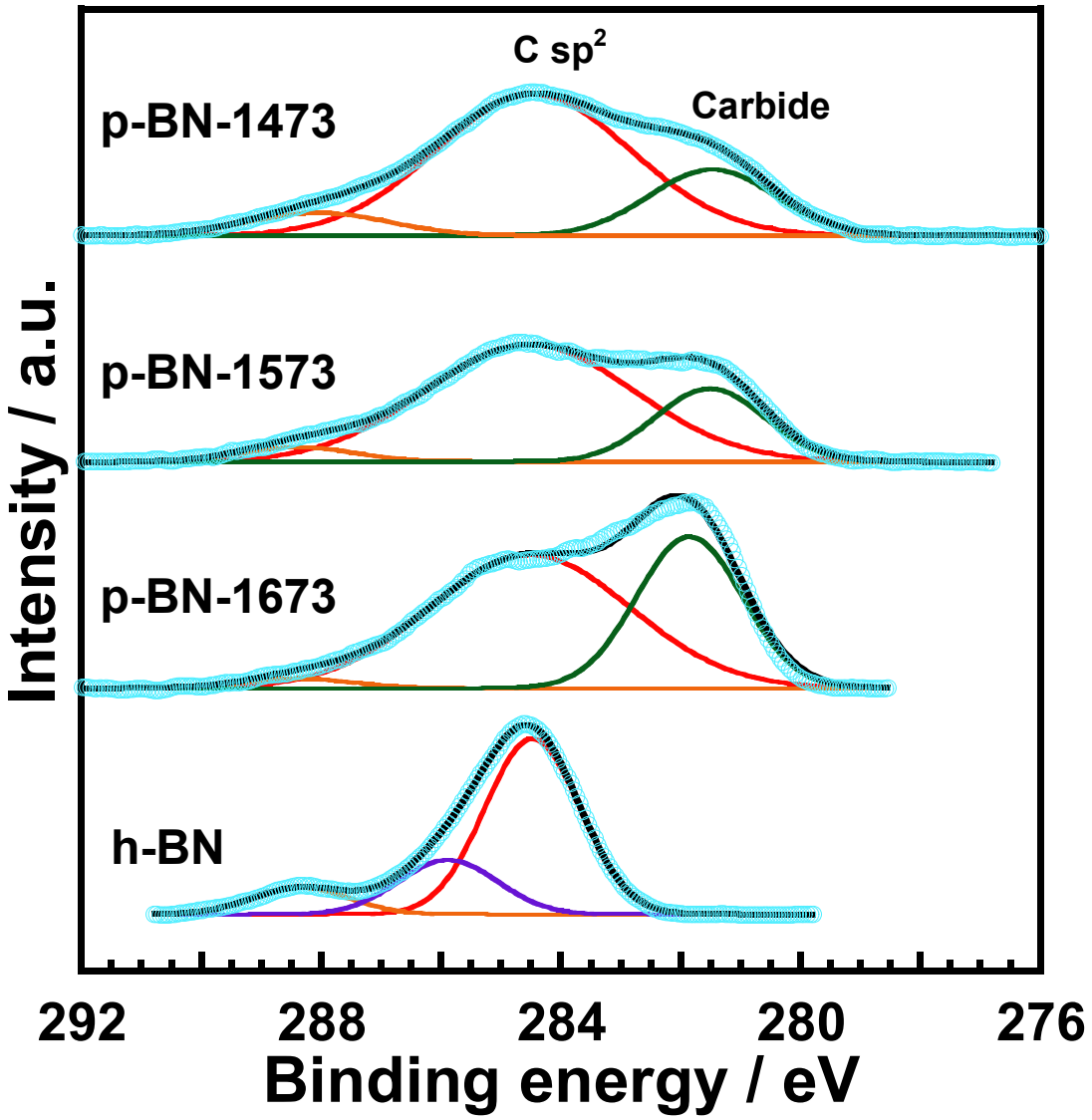

Fig. S5 C 1s XPS spectra of p-BN-*x* and *h*-BN. Here, blue dots and black lines denote experimental and sum of the components in curve fitting procedures, respectively.

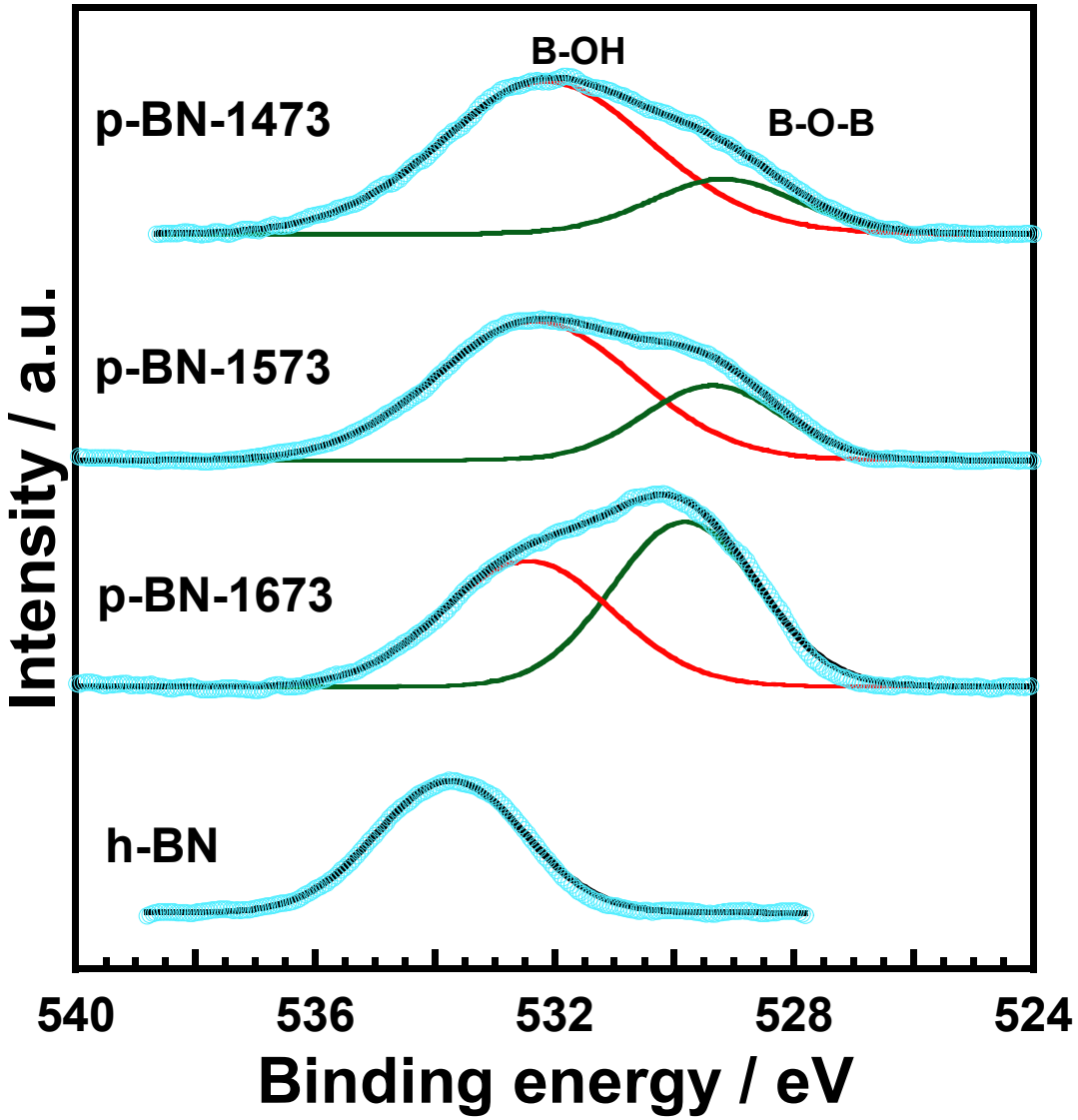

Fig. S6 O 1s XPS spectra of p-BN and *h*-BN. Here, blue dots and black lines denote experimental and sum of the components in curve fitting procedures, respectively.

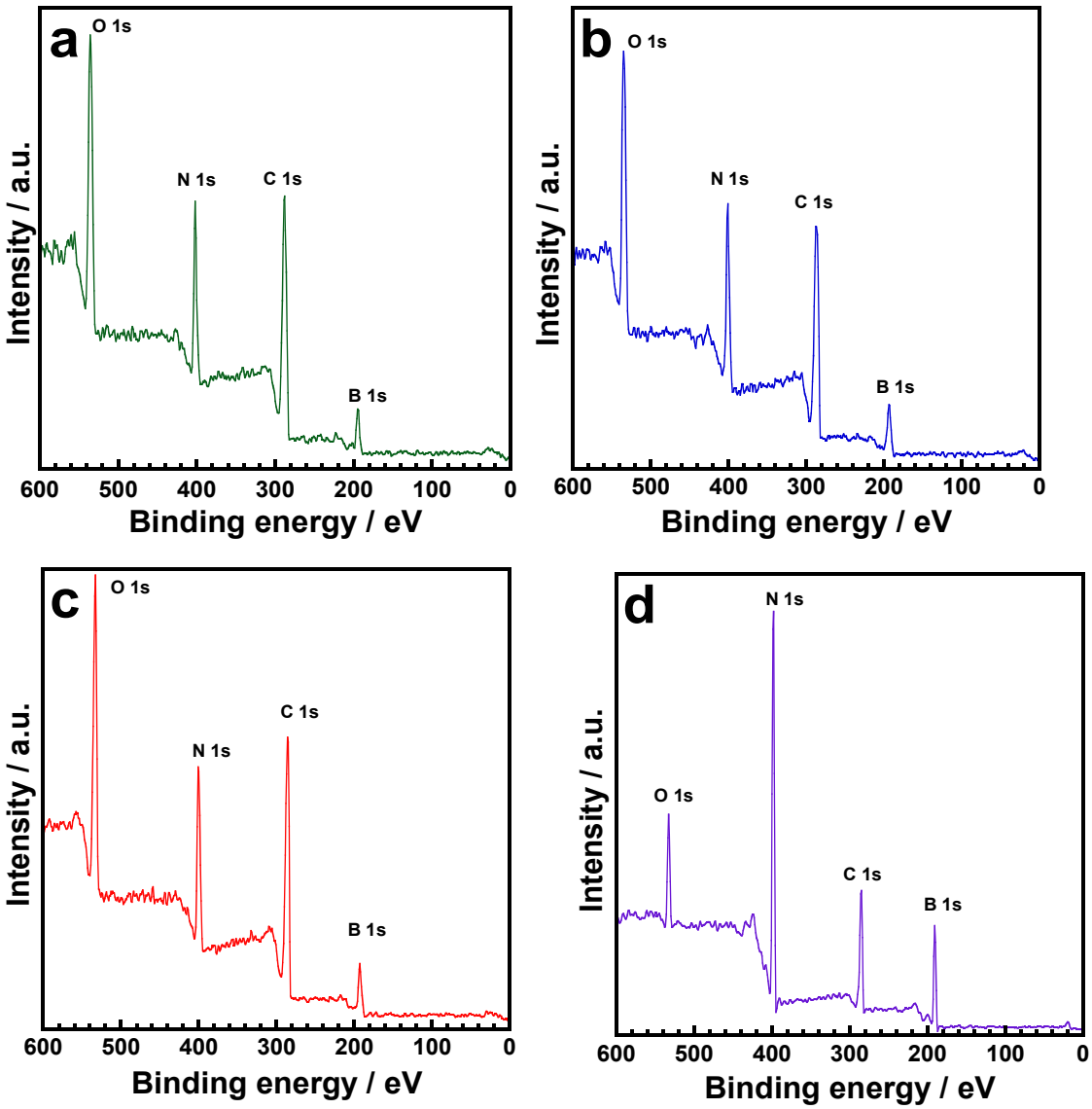

Fig. S7 Wide-energy-range XPS spectra of (a) p-BN-1473, (b) p-BN-1573, (c) p-BN-1673, and (d) *h*-BN.

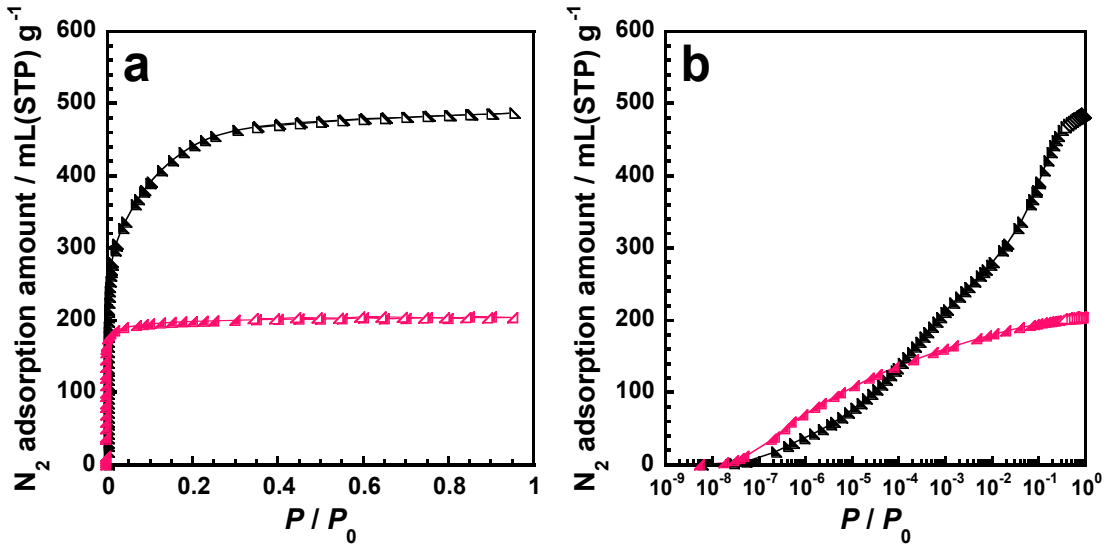

Fig. S8 Adsorption-desorption isotherms of N_2 at 77 K in (a) linear and (b) logarithmic scales on A7 (pink) and A20 (black).

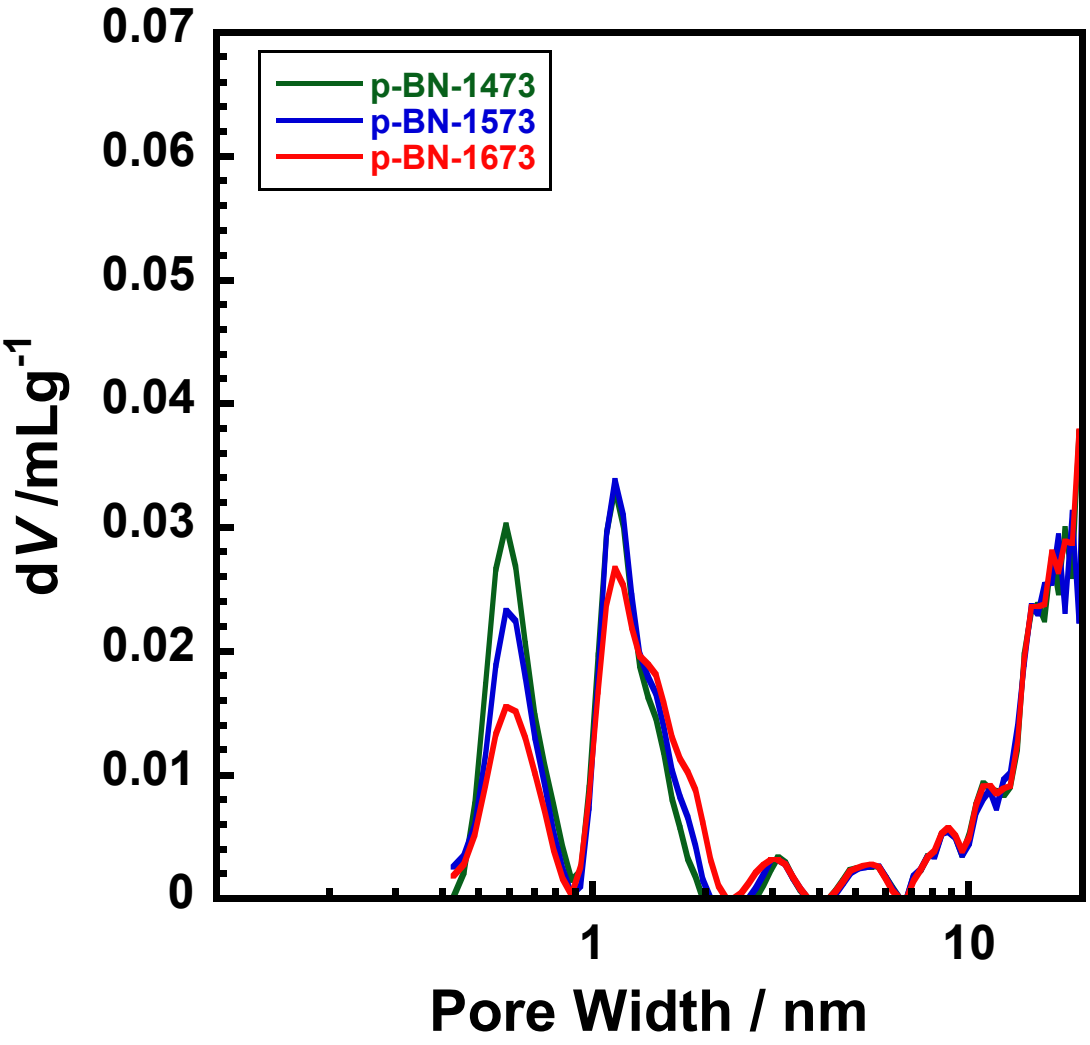

Fig. S9 Pore size distributions of p-BN-1473 (green), p-BN-1573 (blue) and p-BN-1673 (red).

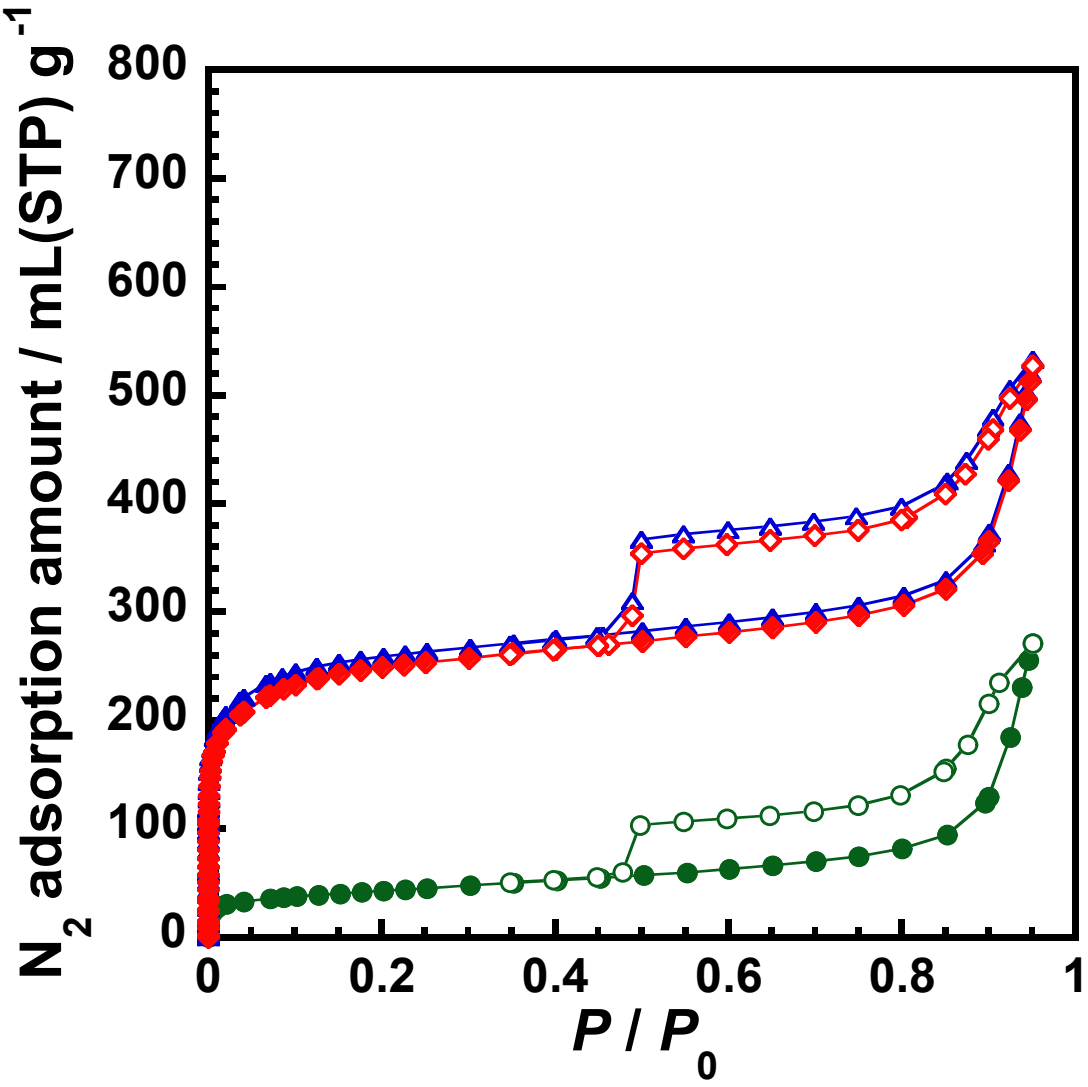

Fig. S10 Adsorption-desorption isotherms N_2 at 77 K on p-BN-1473-ox (green), p-BN-1573-ox (blue) and p-BN-1673-ox (red).

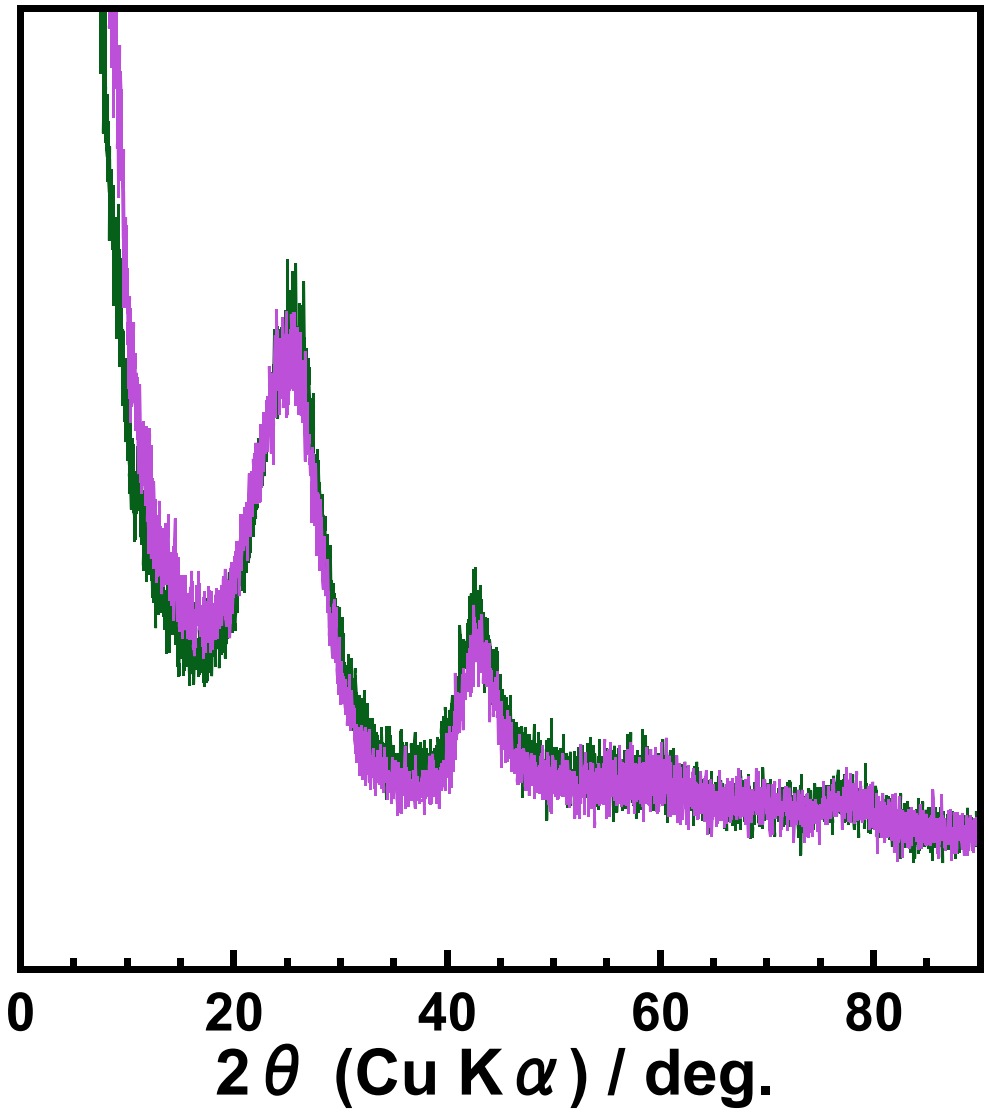

Fig. S11 Normalized powder XRD profiles of p-BN-1473 before (green) and after (purple) N_2 adsorption.

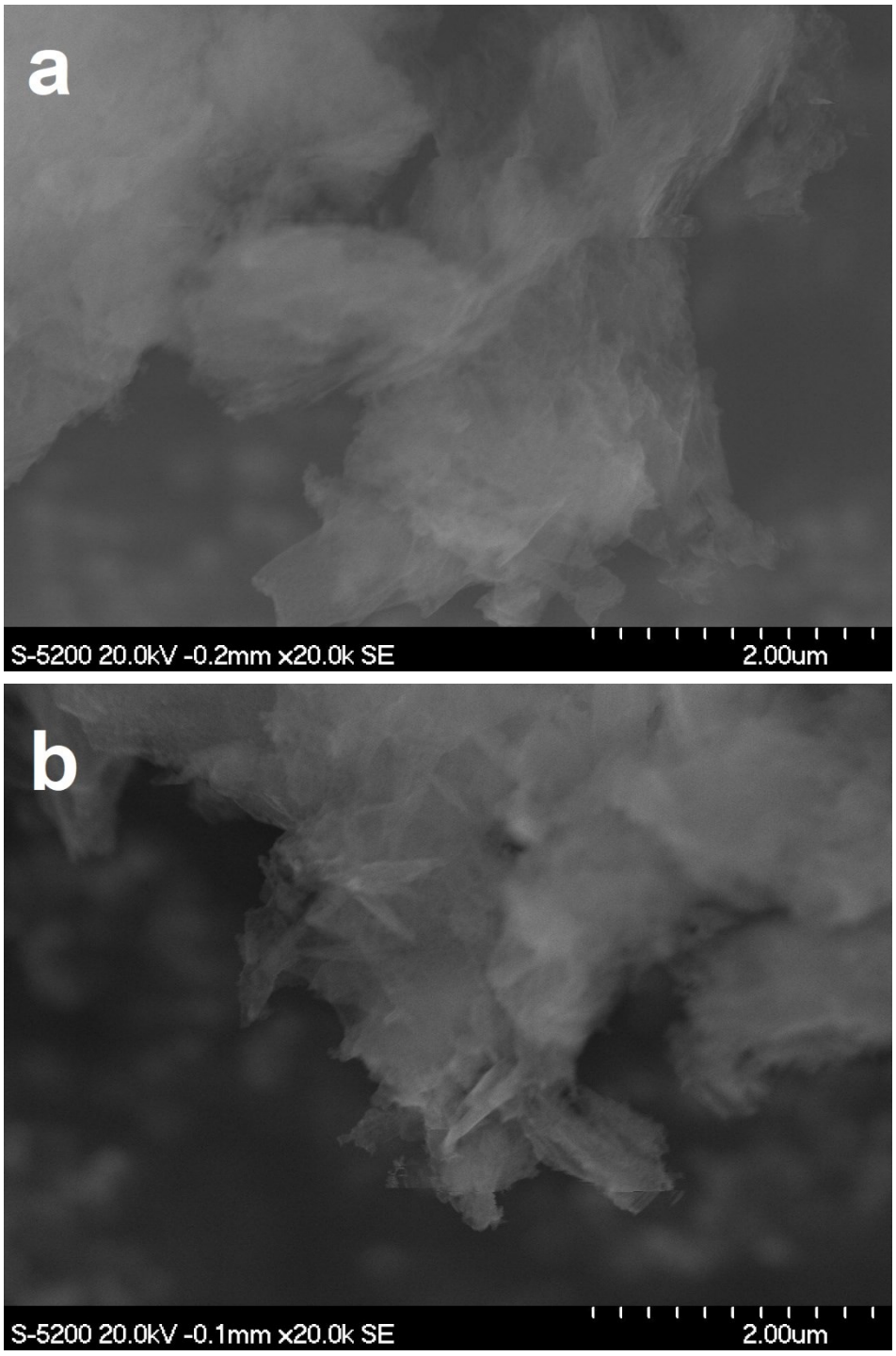

Fig. S12 SEM images of (a) before and (b) after the N_2 adsorption-desorption measurements of p-BN-1473.

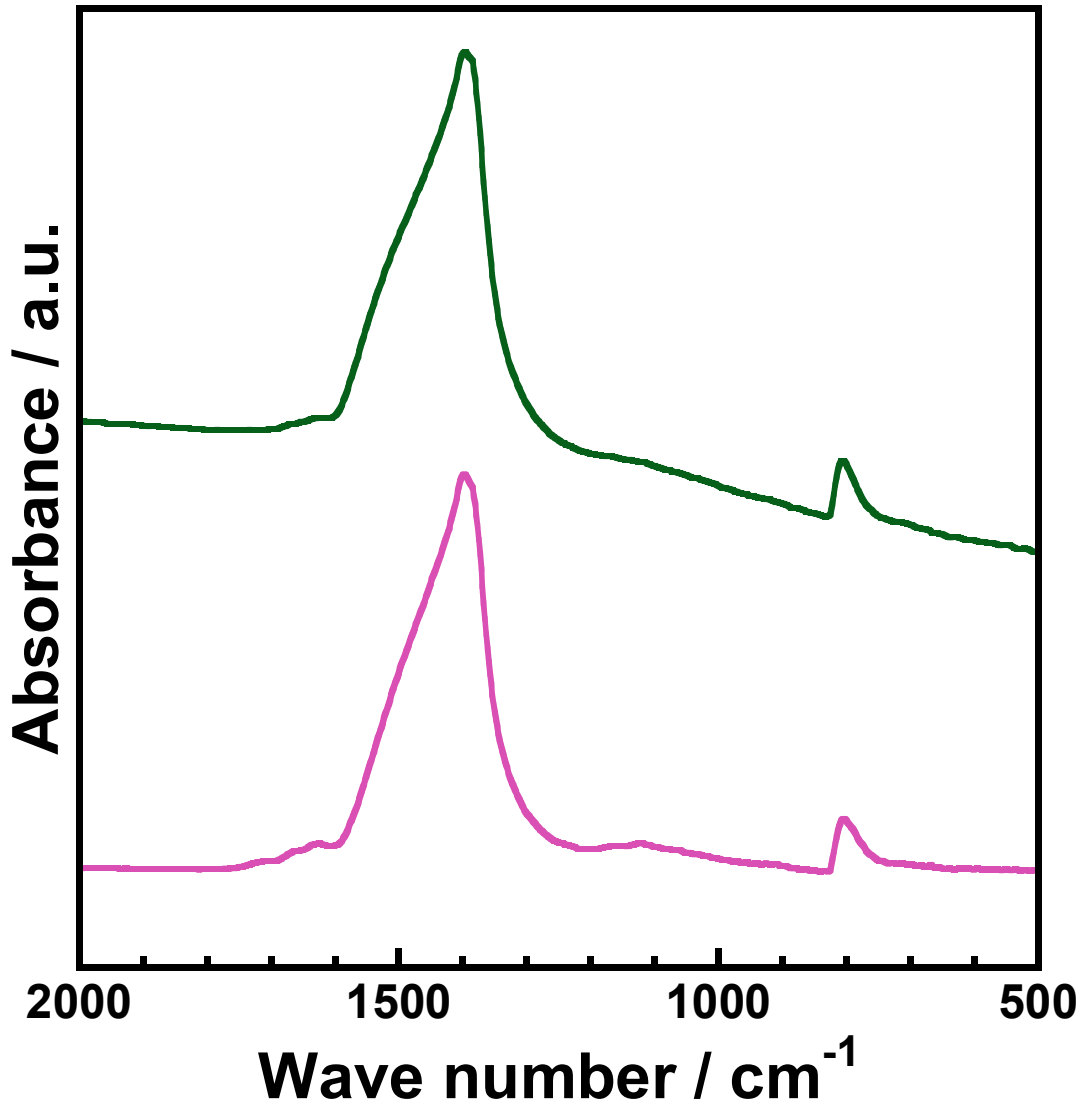

Fig. S13 IR spectra of p-BN-1473 before (green) and after (purple) N_2 adsorption.

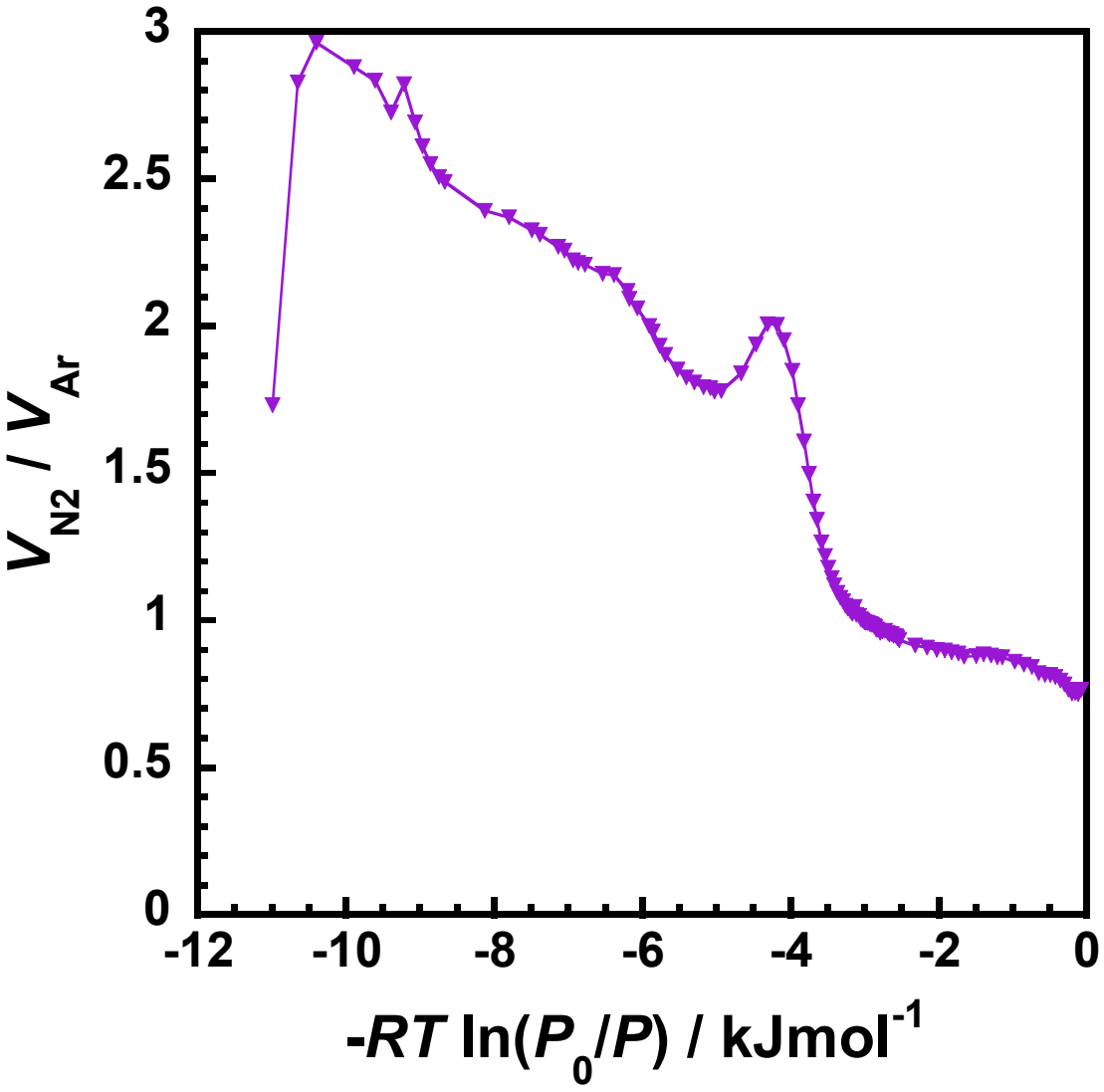

Fig. S14 Relative adsorption amounts of N_2 to Ar on *h*-BN.